Theory of a microscopic maser

P. Filipowicz
Max-Planck-Institute for Quantum Optics, D-8046 Garching bei München, Federal Republic of Germany

J. Javanainen
Department of Physics and Astronomy, University of Rochester, Rochester, New York 14627

P. Meystre
Optical Sciences Center, University of Arizona, Tucson, Arizona 85721
(Received 5 May 1986)

We present the theory of a truly microscopic maser consisting of a single-mode high-Q resonator in which a monoenergetic beam of excited two-level atoms is injected at such a low flux that at most one atom at a time is present inside the cavity. Both a microscopic theory and a heuristic Fokker-Planck approach are presented. We show that the micromaser exhibits a number of novel features that are averaged out in usual masers and lasers. First, the field is in general sub-Poissonian, which reflects the quantization of both the field and its sources. Second, the onset of maser oscillations may be followed by a succession of abrupt transitions in the state of the field. Finally, as the atomic flux through the resonator is increased, the maser threshold acquires characteristics of a continuous phase transition, whereas the subsequent changes in the field distribution become analogous to first-order phase transitions.

I. INTRODUCTION

Resonator quantum electrodynamics has gained considerable importance in the last few years. Roughly speaking, it can be described as the study of the interaction between one or few atoms or electrons and the electromagnetic fields that can be realized in particular in high-Q microwave cavities or in traps. Investigations along these lines have and will allow the observation of order-of-magnitude effects of the quantized nature of the electromagnetic field, such as, e.g., a modification of the spontaneous lifetime of a transition in a tailored electromagnetic field environment,[1-3] Lamb-shift corrections,[4] etc.[5]

For many years, theorists have analyzed various aspects of the Jaynes-Cummings model[6] of a single atom in interaction with a single mode of the electromagnetic field. A number of predictions, including the existence of the so-called "Cummings collapse"[7-9] and "revivals"[10] have been made, whose existence is a signature of the truly quantum-mechanical nature of the field. But it is only recently that the experimental possibilities have reached the point where such systems can actually be realized.[1,2,11] This breakthrough is based on the combined advantages of Rydberg-state spectroscopy and of superconducting microwave cavities of extremely high-Q factors ($Q=10^9$ and higher). It is now possible to build microscopic systems that exhibit the genuine quantum-mechanical dynamics generally masked by unavoidable fluctuations in their macroscopic counterparts. These new developments have led, in the last few months, to the first observation of the Cummings collapse and revivals.[12]

Thus, what was once thought to be just a rather unrealistic theoretical testing ground for basic ideas on the foundations of quantum optics is now within the reach of experimental tests. There are strong indications[13] that systems closely related to those of Refs. 1 and 12 will provide nonclassical sources of radiation.[13-15] On the more fundamental side, they will help shed light on the transition from truly microscopic to macroscopic dynamics in radiation-matter interaction.

In this paper, we present the theory of a truly microscopic maser[11,16] consisting of a single-mode high-Q resonator in which a monoenergetic beam of excited two-level atoms is injected at such a low flux that, at most, one atom at a time is present inside the cavity. We show that it exhibits a number of novel features that are averaged out in usual masers and lasers.[17] First, the field is, in general, sub-Poissonian, which reflects the quantization of both the field and its sources. Second, the onset of maser oscillations may be followed by a succession of abrupt transitions in the state of the field. Finally, as the atomic flux through the resonator is increased, the maser threshold acquires characteristics of a continuous phase transition, whereas the subsequent changes in the field distribution become analogous to first-order phase transitions.

The rest of this paper is organized as follows. In Sec. II, we present a quantum theory of the micromaser, deriving its steady-state photon statistics and show that it is, in general, sub-Poissonian. The "strong-signal" characteristics are analyzed. We demonstrate how the saturation behavior of conventional lasers is recovered by introducing a sufficient amount of stochasticity in the system. In Sec. III an alternative theory of the micromaser based on a heuristic Fokker-Planck equation is derived. This approach presents a number of advantages over the microscopic theory of Sec. II. In particular, it allows to understand the further transitions past threshold in terms of a

multiple-well potential, in a fashion analogous to the Landau theory of first-order phase transitions. This section concludes with an analysis of the role of atomic fluctuations. Section IV presents the dynamics of the micromaser, based on this Fokker-Planck theory. The intrawell redistribution time and interwell tunneling time are evaluated, and it is shown that the typically large value of this last time can lead to hysteretic phenomena in the micromaser. Finally, Sec. V is a summary and discussion.

II. QUANTUM THEORY OF THE MICROMASER

A. Derivation of the photon statistics

We consider a single-mode resonator into which excited two-level atoms are injected at a rate low enough that at most one atom at a time is inside the resonator. In addition, we assume that the atom-field interaction time $t_{\rm int}$ is much shorter than the cavity damping time γ^{-1}, so that the relaxation of the resonator field mode can be ignored while an atom is inside the cavity.[18] The strategy to describe the maser is then straightforward: While an atom flies through the cavity, the coupled field-atom system is described by the Jaynes-Cummings Hamiltonian, and during the intervals between successive atoms the evolution of the field is governed by the master equation of a harmonic oscillator interacting with a thermal bath.

The Jaynes-Cummings Hamiltonian is[6]

$$H=(\hbar\omega_0/2)S_3+\hbar\omega a^\dagger a+(\hbar\kappa/2)(S_+a+S_-a^\dagger)\ , \tag{2.1}$$

where ω_0 is the frequency difference between the two atomic levels, κ the electric dipole coupling constant, a and $a^\dagger$ the annihilation and creation operators, ω the frequency of the cavity field mode, and $S_3, S_\pm$ are the standard Pauli spin operators. The Jaynes-Cummings Hamiltonian is exactly solvable, and the corresponding time evolution operator $U(t)=\exp(-iHt/\hbar)$ is well known.[6-10]

At time t_i, the ith atom enters the cavity containing the field described by the density operator $\rho_f(t_i)$. At this time, the density operator ρ of the combined atom-field system is simply the tensor product of $\rho_f(t_i)$ and of the initial atomic density operator. After the interaction time $t_{\rm int}$ the atom exits the resonator, and leaves the field in the state described by the reduced density operator

$$\begin{aligned}\rho_f(t_i+t_{\rm int})&={\rm Tr}_a[U(t_{\rm int})\rho(t_i)U^\dagger(t)]\\&\equiv F(t_{\rm int})\rho_f(t_i)\ ,\end{aligned} \tag{2.2}$$

where ${\rm Tr}_a$ stands for trace over the atomic variables.

In the interval between $t_i+t_{\rm int}$ and the time t_{i+1} at which the next atom is injected, the field evolves at rate γ towards a thermal steady state with a temperature-dependent mean photon number n_b, as described by the standard master equation[19]

$$\begin{aligned}\dot\rho_f\equiv L\rho_f&=(\gamma/2)(n_b+1)(2a\rho_f a^\dagger-a^\dagger a\rho_f-\rho_f a^\dagger a)\\&+(\gamma/2)n_b(2a^\dagger\rho_f a-aa^\dagger\rho_f-\rho_f aa^\dagger)\end{aligned} \tag{2.3}$$

of a damped harmonic oscillator.

Hence, at time t_{i+1} the field density matrix is given by

$$\rho_f(t_{i+1})=\exp(Lt_p)F(t_{\rm int})\rho_f(t_i)\ , \tag{2.4}$$

where $t_p=t_{i+1}-t_i-t_{\rm int}\simeq t_{i+1}-t_i$ is the time interval between atom i leaving the resonator and atom $i+1$ entering it.

Suppose that the field density matrix is initially diagonal in the number state representation, and that atoms without initial coherence are injected inside the resonator. The reduced density operator of the field then remains diagonal during the interaction, $\langle n\,|\,\rho_f\,|\,n'\rangle=p_n\delta_{n,n'}$. In component form, Eq. (2.2) reduces to

$$p_n(t_i+t_{\rm int})=(1-\beta_{n+1})p_n(t_i)+\beta_n p_{n-1}(t_i)\ , \tag{2.5}$$

where the factors[6]

$$\beta_n=\frac{n\kappa^2}{\Delta^2+n\kappa^2}\sin^2[\tfrac{1}{2}(\Delta^2+n\kappa^2)^{1/2}t_{\rm int}] \tag{2.6}$$

reflect the coherent nature of the atom-field interaction. Here $\Delta=\omega-\omega_0$ is the usual atom-field detuning. Moreover, the diagonality of the field is preserved during its decay, so that the master equation (2.3) can be restricted to its diagonal elements:

$$\begin{aligned}\dot p_n&=\gamma(n_b+1)[(n+1)p_{n+1}-np_n]\\&+\gamma n_b[np_{n-1}-(n+1)p_n]\ .\end{aligned} \tag{2.7}$$

Under these conditions, successive iterations of Eq. (2.4) eventually yield a diagonal steady-state field density matrix $\rho_{r,\rm st}$, which is the solution of this equation with $\rho_f(t_{i+1})=\rho_f(t_i)$. Note that this is not a "true" steady state, but rather a steady state of the return map (2.4). Physically, it corresponds to a situation where the same field repeats at the precise instants when successive atoms exit the cavity.

In the remainder of this paper, we always consider exact resonance $\Delta=0$. For the time being, we also assume that the atoms enter the cavity according to a Poisson process with mean spacing $1/R$ between events, where R is the atomic flux. We discuss in detail the implications of this model in Sec. III. The Appendix shows that the stochastic average of the field over the random spacings of the $i+1$ atoms, $\bar\rho_f^{\,i+1}$, is still related to the average after i atoms by a return map of the type (2.4), except that the damping operator $L(t_p)$ is replaced by its average $(1-L/R)^{-1}$ over the exponential distribution $P(t_p)=R\exp(-Rt_p)$ of the intervals between atoms. Equation (2.4) then becomes

$$\bar\rho_f(t_{i+1})=(1-L/R)^{-1}F(t_{\rm int})\bar\rho_f(t_i)\ . \tag{2.8}$$

With the injection of a succession of atoms inside the cavity, the stochastic average of the field density matrix evolves towards a steady state $\bar\rho_{f,\rm st}$ satisfying the relation

$$(1-L/R)\bar\rho_{f,\rm st}=F(t_{\rm int})\bar\rho_{f,\rm st}\ . \tag{2.9}$$

With the aid of (2.5) and (2.7), (2.9) yields a three-term recursion relation for the occupation numbers $\bar p_n\equiv\langle n\,|\,\bar\rho_{f,\rm st}\,|\,n\rangle$, which may be expressed in the form

$$S_n=S_{n+1}\ , \tag{2.10a}$$

with

$$S_n \equiv N_{\rm ex}\beta_n \bar{p}_{n-1} + n_b n \bar{p}_{n-1} - (n_b+1) n \bar{p}_n \ . \quad (2.10b)$$

Here,

$$N_{\rm ex} \equiv R/\gamma \quad (2.11)$$

is the average number of atoms that traverse the cavity during the lifetime of the field. The physical condition that the field density matrix be normalizable implies that $\bar{p}_n \to 0$ faster than $1/n$ for $n \to \infty$. Hence, $S_n \to 0$ for $n \to \infty$, and from Eq. (2.10a) one has readily $S_n = 0$ for all n. Equation (2.10b) then gives the ratio of successive occupation numbers,

$$\bar{p}_n = \frac{n_b}{1+n_b}\left[1+\frac{N_{\rm ex}\beta_n}{n n_b}\right]\bar{p}_{n-1}, \quad n=1,2,\ldots, \quad (2.12)$$

from which the analytic expression of the steady-state occupation numbers follows up to a normalization constant:[16]

$$\bar{p}_n = C\left[\frac{n_b}{1+n_b}\right]^n \prod_{k=1}^{n}\left[1+\frac{N_{\rm ex}}{n_b}\frac{\beta_k}{k}\right] . \quad (2.13)$$

This is the central result of this paper. In the remainder of Sec. II, we show that it implies that the micromaser exhibits a number of features absent from conventional lasers and masers. Section III then presents an alternative, approximate theory that sheds new light on a number of the unusual aspects of this system.

B. Features of the photon statistics

Since the intracavity field always remains diagonal, the photon statistics (2.13) contains all information about the statistical properties of the steady-state field reached by the micromaser. The approach to steady state, which is given by Eq. (2.8), is not itself amenable to an analytical solution and requires from the onset a numerical analysis. This section discusses both the physical implications of the steady-state result (2.13) and the approach to equilibrium.

Figure 1 shows the normalized average number of photons $l \equiv \langle n \rangle / N_{\rm ex}$, where

$$\langle n \rangle = \sum_{k=1}^{\infty} k \bar{p}_k \ , \quad (2.14)$$

as a function of the dimensionless parameter θ defined as

$$\theta = (N_{\rm ex})^{1/2} \kappa t_{\rm int}/2 \ . \quad (2.15)$$

Later on we show that θ plays the role of a pump parameter for the micromaser.

The three curves correspond to $N_{\rm ex}=20$, 200, and 2000, and the number of thermal photons is $n_b = 0.1$. A common feature to all cases is that l is nearly zero for small θ, but a finite l (and $\langle n \rangle$) emerges at the threshold value $\theta = 1$. For θ increasing past this point, l first grows rapidly, but then decreases to reach a minimum at about $\theta \simeq 2\pi$, where the field abruptly jumps to a higher intensity. This general behavior recurs roughly at integer multiples of 2π, but becomes less pronounced for increasing θ.[20] Finally, a

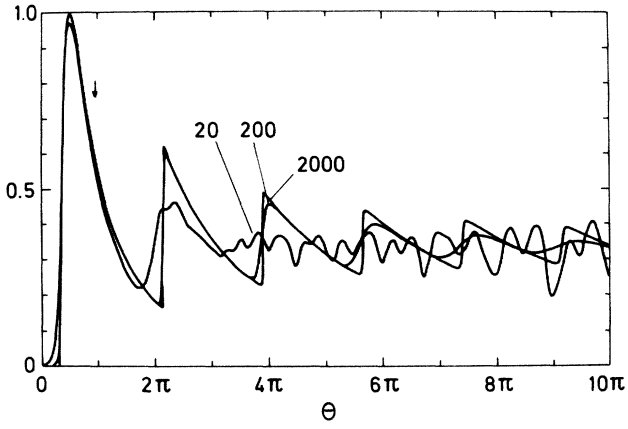

FIG. 1. Normalized steady-state photon number l as a function of the pump parameter θ for $N_{\rm ex}=20$, 200, 2000, and a blackbody photon number $n_b = 0.1$.

stationary regime with l nearly independent of θ is reached. Outside the time scale of Fig. 1 there is still additional structure reminiscent of the Jaynes-Cummings revivals.[10,12,16]

The number and, in particular, the sharpness of the features in the photon number depend on $N_{\rm ex}$. At the onset of the field around $\theta = 1$ the function $l(\theta)$ essentially does not depend on $N_{\rm ex}$ if $N_{\rm ex} \gg 1$, but the subsequent transitions becomes sharper for increasing $N_{\rm ex}$. In the limit $N_{\rm ex} \to \infty$, this hints at an interpretation of the first transition in terms of a continuous phase transition, while the others are similar to first-order phase transitions.

It is possible to give a simple interpretation of the first transition (threshold) of the micromaser in terms of a gain-loss argument reminiscent of conventional laser-maser theory.[17] In the spirit of a "rate-equation" analysis, one would expect the average number of photons in the cavity mode to be governed by an equation of the form

$$\langle \dot{n} \rangle = \gamma N_{\rm ex} \sin^2(\kappa \sqrt{\langle n+1 \rangle} t_{\rm int}/2) - \gamma \langle n \rangle \ . \quad (2.16)$$

The first term in Eq. (2.16) is the gain due to the change in atomic inversion as deduced from the Rabi oscillations formula, where we have used (2.11) and the "+1" accounts for spontaneous emission into the resonator mode, while the second term describes cavity losses (here $n_b = 0$). The possible mean photon numbers $\langle n \rangle$ are approximately given by the stable stationary solutions of Eq. (2.16). For $\theta \ll 1$ the only solution for the field is $\langle n \rangle \simeq \theta^2 \ll 1$. The maser threshold occurs when the linearized (stimulated) gain for $\langle n \rangle \simeq 0$ compensates the cavity losses:

$$\gamma N_{\rm ex} \frac{d}{d\langle n \rangle} \sin^2(\kappa \sqrt{\langle n \rangle} t_{\rm int}/2) \Big|_{\langle n \rangle = 0} \simeq \gamma N_{\rm ex} (\kappa t_{\rm int})^2/4 = \gamma \ , \quad (2.17)$$

which reduces precisely to the threshold value $\theta = 1$ obtained from the exact photon statistics (2.13). This justifies interpreting θ as the pump parameter of the micromaser.

Figure 2 shows the normalized standard deviation

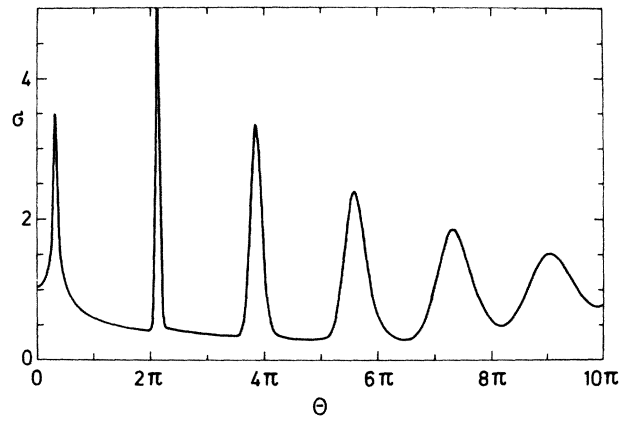

FIG. 2. Normalized standard deviation σ of the photon distribution for $N_{ex}=200$ and $n_b=0.1$. A Poissonian photon distribution corresponds to $\sigma=1$.

$$\sigma \equiv \frac{(\langle n^2\rangle - \langle n\rangle^2)^{1/2}}{\langle n\rangle^{1/2}} \tag{2.18}$$

of the photon distribution as a function of θ for $N_{ex}=200$ and $n_b=0.1$. Above the threshold $\theta=1$ the photon statistics is first strongly super-Poissonian, with $\sigma\simeq 4$. (Poissonian photon statistics would yield $\sigma=1$.) Further super-Poissonian peaks occur at the positions of the subsequent transitions. In the remaining intervals of θ, σ is typically of the order of 0.5, a signature of the sub-Poissonian nature of the field.

The first two moments are instructive in that they give an at-a-glance characterization of the photon statistics, but naturally they do not describe it completely. Figure 3 shows the steady-state photon number distribution $\bar{p}_n$ for $N_{ex}=200$ and $n_b=0.1$ for two values of the pump parameter $\theta=3\pi$ and 15π. For $\theta=3\pi$ a clean sub-Poissonian photon statistics emerges, whereas for 15π the distribution has multiple peaks. Far above threshold, the micromaser does not tend towards the Poissonian photon statistics typical of conventional single-mode, homogeneously broadened lasers. Section II C shows how these results can be recovered.

Figure 4 illustrates the time evolution of the intracavity field mode and its approach to equilibrium for $N_{ex}=50$ and $n_b=1$. The initial photon statistics characteristic of a thermal field evolve in time to a multiple-peaked, irregular structure somewhat reminiscent of the field found in the Jaynes-Cummings model,[21] despite the fact that in this last case, no steady state is reached.

C. Recovering the ordinary maser

The photon statistics of the microscopic maser exhibits features alien to ordinary masers and lasers: The field is typically strongly "nonclassical." (By classical field, we mean a field with a positive-definite Glauber-Sudarshan P representation.[22]) It has no particular tendency, even far above threshold, of being Poissonian (Glauber coherence), and extra phase transitions take place when the pump parameter is increased. In this section, we show that the differences between our conclusions and traditional laser theories arise because our microscopic maser possesses *less* stochasticity and noise than macroscopic masers and lasers. As a result, the quantum-mechanical phases characteristic of the coherent light-matter interaction are not lost or averaged over, and they affect the steady state of the system.

Of course, we have introduced some noise with the averaging over the intervals t_p between atoms. But because many atoms traverse the cavity during the lifetime of the field, this noise has little influence on the qualitative results, as discussed below. As a matter of fact, this average is primarily a technical trick to obtain the analytic form (2.13) of the photon statistics. Another source of noise is associated with cavity damping, as implied by the fluctuation-dissipation theorem. The major effect of this damping is to force the evolution of the system towards a steady state. In a recent paper,[15] we showed that there are

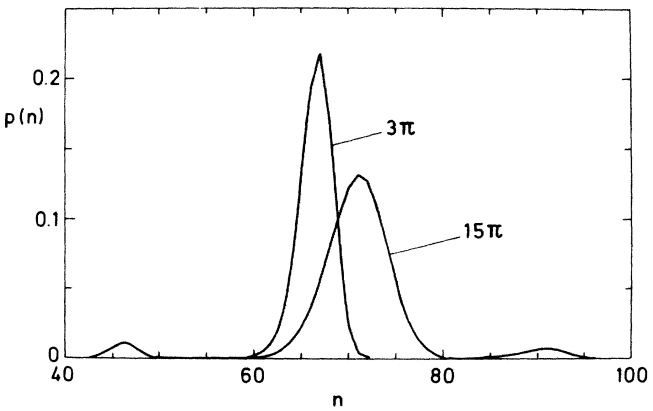

FIG. 3. Steady-state photon statistics for $N_{ex}=200$, $n_b=0.1$, and $\theta=3\pi$ and 15π, these last values labeling the curves. Note the three-peaked distribution for $\theta=15\pi$.

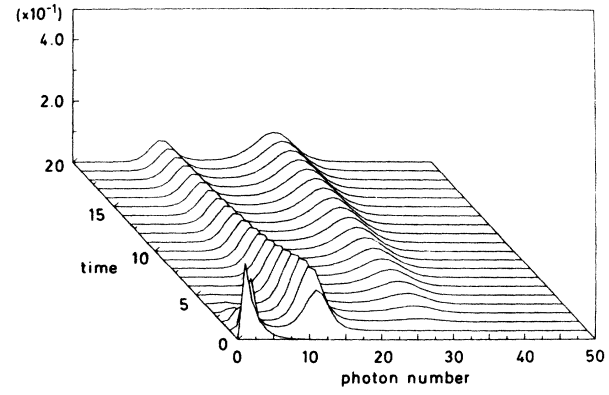

FIG. 4. Time evolution of the field photon statistics for $N_{ex}=50$ and $n_b=1.0$, evolving from thermal to a two-peaked steady-state distribution. Time in units of the inverse cavity damping rate γ.

some situations, albeit nongeneric, where an idealized micromaser can reach a steady state even in the absence of losses. In such cases, the steady-state field is either a truncated inverted thermal distribution (negative temperature), or a pure number state, i.e., a field of even "less" classical nature than the micromaser described here.

A classical field, and specifically Poissonian photon statistics far above threshold, are reached only if a *sufficient* amount of stochasticity is added to the model. To prove this point, we introduce a distribution of atomic velocities, i.e., a distribution of the interaction times $t_{\rm int}$. As argued in the Appendix, a correct way to do this in the case when the interaction times of successive atoms are statistically independent is to average the operator $F(t_{\rm int})$ on the right-hand side (rhs) of (2.4) over $t_{\rm int}$, which boils down to averaging the factors $\beta_k(t_{\rm int})$ in (2.13). For simplicity we assume that the distribution of the interaction times is a Gaussian with mean $\bar{t}_{\rm int}$ and rms spread δt. The factors β_k in (2.13) are then to be replaced by

$$\bar{\beta}_k = \tfrac{1}{2}[1 - e^{-k(\kappa\delta t)^2/2}\cos(\kappa k \bar{t}_{\rm int})] \ . \tag{2.19}$$

Figure 5 shows the mean number of photons for $N_{\rm ex}=200$ and $n_b=0.1$ as a function of the pump parameter θ corresponding to the average interaction time $\bar{t}_{\rm int}$, for three values of the relative spread of the interaction times $\delta t/\bar{t}_{\rm int}=0$, 0.1, and 1. The first few transitions survive a 10% spread of the interaction times, but all features except the maser threshold are washed out when the relative spread mimics a thermal atomic beam, $\delta t/\bar{t}_{\rm int}=1$.[20] In fact, at $\theta \simeq 2\pi$ corresponding to the first transition the argument inside the exponential of (2.19) is then already of the order of -10, and the term proportional to the exponential is negligible. The photon number distribution thus reduces to

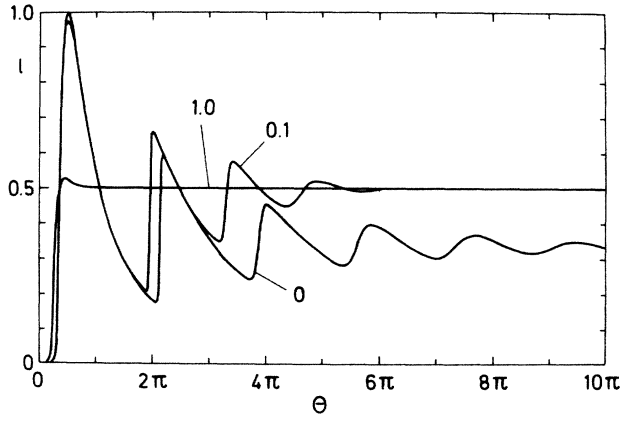

FIG. 5. Effect of an interaction time (or atomic velocity)0 distribution on the normalized average photon number $I(\theta)$. The interaction times are taken to have a Gaussian distribution of mean $\bar{t}_{\rm int}$ and normalized standard deviation $\delta t/\bar{t}_{\rm int}=0$, 0.1, and 1, these values labeling the curves. The other parameters are $N_{\rm ex}=200$ and $n_b=0.1$.

$$\bar{p}_n = C\left[\frac{n_b}{1+n_b}\right]^n \prod_{k=1}^{n}\left[1+\frac{N_{\rm ex}}{2n_b k}\right], \tag{2.20}$$

and far above threshold, $N_{\rm ex}\gg 1$, this gives the Poisson distribution

$$p_n = C\left[\frac{N_{\rm ex}}{2(1+n_b)}\right]^n \frac{1}{n!} \ . \tag{2.21}$$

Thus, a (classical) incoherent average is needed to obtain Poissonian photon statistics. The reason is that the granulated character of the quantum-mechanical phases involved in the coherent atom-field dynamics is averaged over. Hence the field no longer supplies to the atom a reaction which depends strongly on its state, so that the electrons in the atoms act much like a classical current.[22] A sufficient amount of inhomogeneous broadening, with a concomitant averaging over the detuning Δ in Eq. (2.13), would produce the same result.

The same general argument also holds true in the conventional single-mode, homogeneously broadened laser, except that in this case it is an incoherent average over the radiative lifetime of the laser levels that leads to the smoothing of the quantum-mechanical phases.[17] The fundamental difference between these two situations is that the irreversible spontaneous emission, unavoidable in optical resonators, looses its meaning in the microscopic maser. In this case, the atoms interact truly with a single mode of the electromagnetic field. There is no continuum of field modes for the system to decay into, and no irreversible spontaneous emission. From this point of view, the (usually) sub-Poissonian output of the microscopic maser can be seen as a consequence of inhibited spontaneous emission.[2,3] Conventional lasers and masers are essentially classical systems; the micromaser is not.

III. FOKKER-PLANCK APPROACH

So far we have carried out an exact quantum theory of the microscopic maser. Further insight into the physical origin and nature of the unconventional photon statistics and phase transitions in this system can be gained by a semiheuristic approach in terms of a Fokker-Planck equation. We shall find that for large $N_{\rm ex}$ and n_b not too small, this approximate analysis reproduces and explains to a large extent the results of the exact microscopic theory, and can also be employed to make new predictions about the dynamics of the micromaser.

A. Derivation of an approximate Fokker-Planck equation

Let us temporarily assume that initially exactly $n_0\gg 1$ photons are present in the cavity field mode, and consider the evolution of the photon number in the cavity over a time T long compared to the interaction time $t_{\rm int}$, yet so short that the occupation numbers of the field do not change considerably. Clearly, the assumption $n_0\gg 1$ is not valid near threshold. During the time T, a random number N of initially excited atoms with a Poissonian dis-

tribution of mean $\overline{N}=RT$ traverse the cavity.

Our heuristic model of the micromaser rests on the interpretation that every atom that traverses the cavity has the probability

$$P=\sin^2[(n_0)^{1/2}\kappa t_{\rm int}/2] \tag{3.1}$$

of adding one photon to the field and the probability $1-P$ of leaving it unchanged. Except for a small error introduced by replacing $(n_0+1)^{1/2}$ with $(n_0)^{1/2}$, P is just the probability that an atom which enters the cavity in the excited state leaves it in the ground state. The probability that N atoms add k photons to the field is then given by the familiar binomial formula

$$P_k^N=\begin{bmatrix}N\\k\end{bmatrix}P^k(1-P)^{N-k}\,. \tag{3.2}$$

For precisely N atoms, the average change in photon number $\langle k(N)\rangle_g$ and the average $\langle k^2(N)\rangle_g$ of the square of this change are

$$\langle k(N)\rangle_g=PN \tag{3.3a}$$

and

$$\langle k^2(N)\rangle_g=(P-P^2)N+N^2P^2\,, \tag{3.3b}$$

respectively, as is readily seen by introducing the generating function

$$F(\xi)\equiv\sum_k\begin{bmatrix}N\\k\end{bmatrix}(\xi P)^k(1-P)^{N-k}=(1-P+\xi P)^N\,, \tag{3.4}$$

and noting that

$$\langle k(n)\rangle_g=\left.\frac{dF}{d\xi}\right|_{\xi=1} \tag{3.5}$$

and

$$\langle k^2(N)\rangle_g=\left.\frac{dF}{d\xi}\right|_{\xi=1}+\left.\frac{d^2F}{d\xi^2}\right|_{\xi=1} \tag{3.6}$$

In order to directly compare this approach with the exact quantum mechanical theory of Sec. II, we further average the results (3.3) over Poissonian fluctuations in the arrival times of the atoms. This gives

$$\langle k\rangle_g=P\overline{N} \tag{3.7a}$$

and

$$\langle k^2\rangle_g=P\overline{N}+P^2\overline{N}^2\,, \tag{3.7b}$$

where $\overline{N}=RT$, and we have used $\langle N^2\rangle=\overline{N}^2-\overline{N}$, valid for a Poisson process.

From the master equation (2.7), it is also easy to find the average changes of photon number and of its square due to cavity damping over the time T:

$$\langle k\rangle_d=\gamma T(n_b-n_0)\,, \tag{3.8a}$$

$$\langle k^2\rangle_d=\gamma T(n_0+n_b+2n_0n_b)\,. \tag{3.8b}$$

We assume that gain and decay act independently, so that the corresponding changes in average photon number and rms spread can simply be added:

$$\langle k\rangle=\langle k\rangle_g+\langle k\rangle_d\equiv TQ(n_0)\,, \tag{3.9a}$$

$$(\Delta k)^2=\langle k^2\rangle_p-\langle k\rangle_p^2+\langle k^2\rangle_d-\langle k\rangle_d^2\equiv TG(n_0)\,. \tag{3.9b}$$

To lowest order in T, the functions Q and G are defined as

$$Q(n)=R\sin^2(\sqrt{n}\,\kappa t_{\rm int}/2)-\gamma(n-n_b)\,, \tag{3.10a}$$

$$G(n)=R\sin^2(\sqrt{n}\,\kappa t_{\rm int}/2)+\gamma(n+n_b+2nn_b)\,. \tag{3.10b}$$

We proceed next (somewhat ambiguously) by replacing the photon number distribution p_n by a continuous function $p(n)$, $n\in[0,\infty)$, and extrapolating the short-time evolution given by (3.9) and (3.10) to arbitrary times with the aid of the Fokker-Planck equation

$$\frac{\partial}{\partial t}p(n,t)=-\frac{\partial}{\partial n}[Q(n)p(n,t)]+\frac{1}{2}\frac{\partial^2}{\partial n^2}[G(n)p(n,t)]\,. \tag{3.11}$$

The "justification" of this choice of Fokker-Planck equation is that for an initial photon distribution of the form $p(n)=\delta(n-n_0)$, corresponding physically to $p_n=\delta_{n,n_0}$, the short-time evolution of the average photon number and of its rms deviation obtained from (3.11) coincide with (3.9). But there is no *a priori* guarantee that the Fokker-Planck description will give satisfactory results for long times, and only a direct comparison with the results of Sec. II will be able to test its reliability.

A few comments of a general nature can however already be made at this point. The derivation of the moments (3.9) shows that the Fokker-Planck equation (3.11) can be expected to be valid only if the relative changes of the functions $F(n)$ and $G(n)$ are small when n is changed by unity. First, it cannot be trusted for small n. Second, the condition that the argument of the sine in the Rabi flopping factor P in (3.1) should change by much less than unity when n changes by unity can be written as

$$\frac{\kappa t_{\rm int}}{4\sqrt{n}}\ll 1\,, \tag{3.12}$$

or equivalently

$$\theta\ll(nN_{\rm ex})^{1/2}\,. \tag{3.13}$$

Since the quantum theory of Sec. II shows that $\langle n\rangle\lesssim N_{\rm ex}$, these requirements imply that the Fokker-Planck theory can be applied only when $N_{\rm ex}\gg 1$.

In view of this discussion, we scale time to the cavity damping time $1/\gamma$ and photon numbers to $N_{\rm ex}$, a procedure that becomes exact in the limit $N_{\rm ex}\to\infty$, or more precisely $n_b/N_{\rm ex}\to 0$:

$$\tau=t\gamma\,, \tag{3.14a}$$

$$\nu=\frac{n}{N_{\rm ex}}\,. \tag{3.14b}$$

The Fokker-Planck equation then reads as

$$\frac{\partial}{\partial\tau}p(\nu,\tau)=-\frac{\partial}{\partial\nu}[q(\nu)p(\nu,\tau)] + \frac{1}{2N_{ex}}\frac{\partial^2}{\partial\nu^2}[g(\nu)p(\nu,\tau)] , \tag{3.15}$$

with

$$q(\nu)\simeq\sin^2(\sqrt{\nu}\theta)-\nu \tag{3.16a}$$

and

$$g(\nu)\simeq\sin^2(\sqrt{\nu}\theta)+\nu+2\nu n_b . \tag{3.16b}$$

In these expressions, we have neglected terms n_b/N_{ex}, a procedure valid at finite temperature in the limit $N_{ex}\to\infty$, which is the regime in which the Fokker-Planck approach is expected to become exact. This allows us to scale N_{ex} out of the problem.

B. Stationary solution

The stationary solution to the Fokker-Planck equation (3.11) is

$$p(\nu)=C\frac{1}{g(\nu)}\exp\left[2N_{ex}\int d\nu\frac{q(\nu)}{g(\nu)}\right] , \tag{3.17}$$

where C is a normalization constant. Unfortunately, this result is not normalizable in the internal $(0,\infty)$, which reflects the breakdown of the Fokker-Planck approach at $n\simeq 0$. We therefore utilize it only in the interval $(1/N_{ex},\infty)$ corresponding to the range $(1,\infty)$ of the unscaled photon number n.

Figure 6 shows the average $l(\theta)=\langle\nu(\theta)\rangle$ and Fig. 7 the normalized spread $\sigma(\theta)$ of the intracavity photon number, as deduced from the Fokker-Planck theory (3.17) (dashed lines) and from the microscopic equation (2.13) (solid lines). Here $N_{ex}=200$ and $n_b=1$. The agreement between both analyses is very good except for $\theta\simeq 0$ and above $\theta\simeq 10\pi$, as expected on the basis of the discussion surrounding Eqs. (3.12) and (3.13). It becomes perfect for

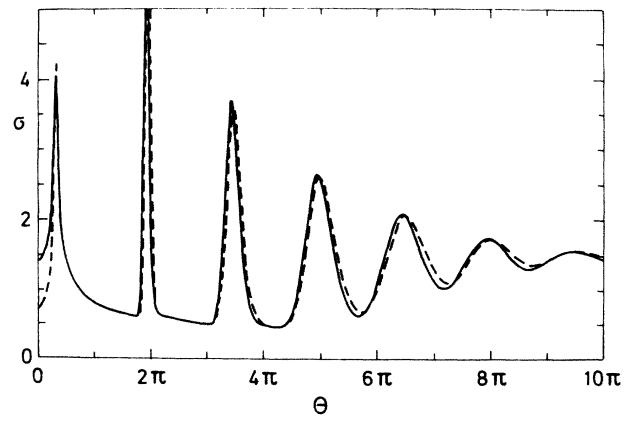

FIG. 6. Comparison of the normalized photon number $l(\theta)$ as obtained from the exact microscopic theory (solid line) and the Fokker-Planck analysis (dashed line). $N_{ex}=200$, $n_b=1$.

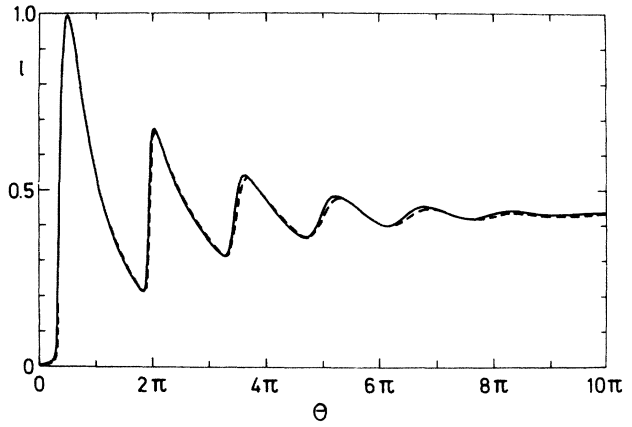

FIG. 7. Normalized standard deviation σ of the field mode photon statistics under the conditions of Fig. 6. Solid line: microscopic theory; dashed line: Fokker-Planck analysis.

$N_{ex}\to\infty$, but for finite N_{ex} deteriorates as n_b is decreased. Still, the qualitative features of the micromaser remain well reproduced by the Fokker-Planck approach as $n_b\to 0$.

Equation (3.17) indicates that for $N_{ex}\gg 1$ the photon-number distribution tends to accumulate in the global minimum of the effective potential

$$V(\nu)=-\int d\nu\frac{q(\nu)}{g(\nu)}=-\int d\nu\frac{\sin^2(\sqrt{\nu}\theta)-\nu}{\sin^2(\sqrt{\nu}\theta)+\nu+2\nu n_b} , \tag{3.18}$$

i.e., near one of the zeros ν_0 of the function $q(\nu)$. Theses zeros are the solutions of

$$\nu_0=\sin^2[(\nu_0)^{1/2}\theta] , \tag{3.19}$$

and which one does correspond to the global minimum of the potential must in general be determined numerically. For the $\theta<1$ the (only) minimum is at $\nu=0$, and the micromaser is below threshold. However, at $\theta=1$ the minimum $\nu=0$ turns into a local maximum. To lowest order in $\theta-1$ the global minimum adjacent to $\nu=0$ is

$$\nu_g=3(\theta-1) . \tag{3.20}$$

When θ grows above unity, the photon number in the cavity mode first increases continuously from zero as illustrated in Fig. 1. As already discussed, this is because at the threshold $\theta=1$ the gain overtakes the losses, and maser oscillations follow. As in conventional lasers, this process is analogous to a continuous phase transition.[23]

As θ is further increased, the effective potential $V(\nu)$ has an increasing number of minima. This is shown in Fig. 8, where $V(\nu)$ is drawn for the three pump parameters $\theta=4$, $1.058\times 2\pi$, and 8. The intermediate value of θ is precisely such that the global minimum at $\nu=0.167$ is replaced by a global minimum at $\nu=0.647$. It is clear from (3.17) that around this pump parameter the steady-state photon number distribution has to change drastically, which explains the transition at about $\theta=2\pi$ in Fig. 1.

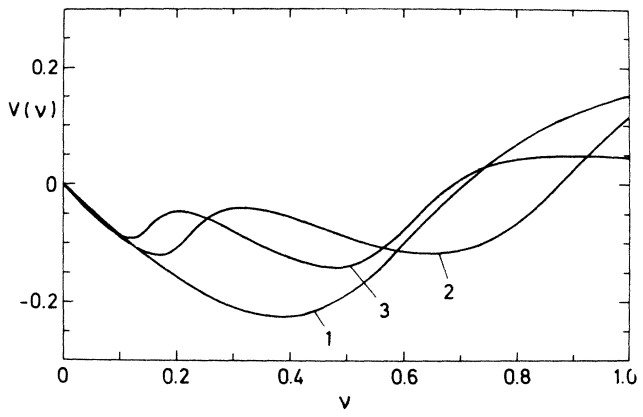

FIG. 8. Potential $V(v)$ in the case $n_b=0$ for the three pump parameters (1) $\theta=4$; (2) $\theta=2.116\pi$; (3) $\theta=8$.

The mechanism of the successive transitions is clearly always the same, with a minimum of $V(v)$ losing its global character and being replaced in this role by the next one. Note that our reasoning is just a variation of the Landau theory of first-order phase transitions, with $\sqrt{v}$ (the field strength, or more precisely the square root of the intracavity intensity) being the order parameter. This analogy supports the notion that in the limit $N_{ex}\to\infty$, these novel features of the micromaser can be interpreted as phase transitions.

Let us finally suppose that the value of the potential $V(v)$ at one of the minima v_g is clearly below its values at other minima, and that $N_{ex}\gg 1$. Then the photon numbers distribution is concentrated close to the global minimum v_g, and in the stationary distribution (3.12) the potential $V(v)$ can be expanded around v_g. This gives

$$p(v)=\frac{C}{g(v_g)}\exp[-N_{ex}(v-v_g)^2V''(v_g)]$$
$$=\frac{C}{2v_g}\exp\left[N_{ex}(v-v_g)^2\frac{q'(v_g)}{2v_g}\right], \tag{3.21}$$

where we have taken for simplicity $n_b=0$ and used $q(v_g)=0$ and $g(v_g)=2v_g$, see Eq. (3.19). The normalized standard deviation (2.18) of the photon numbers becomes

$$\sigma=\left[\frac{-1}{q'(v_g)}\right]^{1/2}, \tag{3.22}$$

independently of the absolute photon numbers. Note that there is no particular reason why (3.22) should in general give $\sigma=1$ pertaining to a Poissonian distribution.

C. The role of fluctuations

In Secs. III A and III B, we have compared a heuristic Fokker-Planck approach with the exact quantum-mechanical description of the micromaser, and introduced a Poisson distribution of atomic arrival times in the derivation of the Fokker-Planck equations (3.11) and (3.15), so as to perform a direct comparison with the closed-form result (2.13). We demonstrated that under well-defined conditions they give practically the same results. On the basis of this comparison, it seems safe to extend the Fokker-Planck approach to cases where the exact treatment does not allow for closed form results. In particular, this section generalizes the Fokker-Planck approach to investigate the influence of various sources of noise on the photon statistics of the micromaser. For simplicity, we restrict ourselves to the case $n_b=0$, keeping in mind that for finite N_{ex}, our analysis will then be qualitative only.

1. Random arrival times

Assume first that the atoms are injected at regular intervals, that is, no Poissonian average is carried out. In this case, the change in photon number due to pumping is governed by (3.3) instead of (3.7). The functions $Q(n)$ and $q(v)$ remain unchanged, but $G(n)$ and $g(v)$ must be modified to give in particular ($n_b=0$)

$$g(v)\to g_1(v)=\sin^2(\sqrt{v}\theta)-\sin^4(\sqrt{v}\theta)+v\ . \tag{3.23}$$

Except for this change, all subsequent calculations go through as before. The positions of the minima of the resulting potential $V_1(v)=-\int dv\,q(v)/g_1(v)$ are clearly the same as the minima of $V(v)$, and some simple algebra based on Eq. (3.19) shows that if v_g is the global minimum of both $V(v)$ and $V_1(v)$, the relative spread of the photon distributions without (σ_1) and with (σ) the Poissonian average are related by

$$\sigma_1=\sigma(1-v_g/2)^{1/2}\ . \tag{3.24}$$

The photon number distribution is narrower without the Poissonian average. Because $v_g<1$, the narrowing cannot be more than by a factor $1/\sqrt{2}$ and is thus of little significance in practice. Still, this result illustrates once more the conclusion of Sec. II: the system becomes more "classical," the more randomness is present in the system. This is further illustrated by considering the effect of an atomic velocity distribution.

2. Atomic velocity distribution

When the interaction time is a random variable, the probability (3.1) that one atom adds a photon to the cavity mode can formally be regarded as a conditional probability for the given interaction time t_{int}. The distribution of interaction times is then accounted for by averaging $P(t_{int})$ over t_{int}, which for a broad velocity distribution gives $\frac{1}{2}$. In this limit, the functions $q(v)$ and $g(v)$ become

$$q_2(v)=\tfrac{1}{2}-v\ , \tag{3.25a}$$

$$g_2(v)=\tfrac{1}{2}+v\ . \tag{3.25b}$$

The corresponding potential $V_2(v)=-\int dv\,q_2(v)/g_2(v)$ has a single minimum at $v_g=\frac{1}{2}$, yielding the average photon number $\langle n_2\rangle=N_{ex}/2$ and the normalized width $\sigma_2=1$. For large average photon numbers, the Gaussian photon number distribution predicted by the Fokker-Planck approach is indistinguishable from a Poissonian distribution extracted from the ordinary laser theory, e.g.,

(2.21). Note that if the Poissonian process for the arrival times had not been assumed, the constants $\frac{1}{2}$ in (3.25) would have been replaced by $\frac{1}{4}$, giving $\sigma_2=\sqrt{3}/2$. Both the assumption abut the Poissonian arrivals and the broad velocity distribution are needed to recover the results of standard laser theory, although the latter has a much more dramatic effect on the photon statistics.

IV. DYNAMICS IN THE FOKKER-PLANCK DESCRIPTION

In the preceding section, we saw that the effective potential $V(\nu)$ typically exhibits a number of local minima. This indicates that the approach to equilibrium of the micromaser will in general be governed by two different time scales. The first one, t_l, rules the redistribution of the photon statistics *inside* a local minimum, and the second one, t_g, gives the tunneling time of the system towards the global minimum of $V(\nu)$. In this section, we evaluate these two times and further show that the multiple-well character of the potential can lead to hysteresis in the state of the field if the pump parameter θ is scanned slowly back and forth.

A. Intrawell redistribution time

Assume first that the initial photon number distribution $p_0(\nu)$ is narrowly peaked about some photon number close to the value ν_m corresponding to one of the minima of the potential $V(\nu)$. For large $N_{\rm ex}$, the minima of $N_{\rm ex}V(\nu)$ are deep and well separated, so that for short enough times, $p(\nu)$ will remain peaked about ν_m, and approach an equilibrium distribution within this well. This intrawell redistribution can be analyzed to a good approximation by neglecting the existence of other minima of $V(\nu)$ altogether, a procedure valid as long as interwell tunneling can be neglected, i.e., that $\tau_l \ll \tau_g$. In this limit, the dynamics of the micromaser is described by the linearized version of the Fokker-Planck equation (3.15):

$$\frac{\partial}{\partial\tau}p(\nu,\tau)=-\frac{\partial}{\partial\nu}[(\nu-\nu_m)q'(\nu_m)p(\nu,\tau)] + \frac{1}{2N_{\rm ex}}\frac{\partial^2}{\partial\nu^2}[g(\nu_m)p(\nu,\tau)] , \tag{4.1}$$

where we have used the result (3.19) that $q(\nu_m)=0$. For a given initial distribution $p_0(\nu)$ the solution of this equation is

$$p(\nu,t)=\int d\nu_0 P(\nu,t;\nu_0,0)p_0(\nu_0) , \tag{4.2}$$

where the propagator P is given by[24]

$$P(\nu,t;\nu_0,0)=\frac{1}{\sqrt{2\pi}u(\tau)}\exp\left[-\frac{[\nu-\nu(\tau)]^2}{2u^2(\tau)}\right] . \tag{4.3}$$

Here

$$u^2(\tau)=\frac{g(\nu_m)}{2N_{\rm ex}q'(\nu_m)}[1-\exp(-2\tau/\tau_l)] , \tag{4.4}$$

$$\nu(\tau)=\nu_m+(\nu_0-\nu_m)\exp(-\tau/\tau_l) , \tag{4.5}$$

and the time constant τ_l is

$$\tau_l=\frac{1}{q'(\nu_m)} . \tag{4.6}$$

Irrespective of the initial distribution $p_0(\nu)$, $p(\nu,\tau)$ evolves over a time scale given by τ_l towards a Gaussian centered at ν_m and with rms spread $u(\infty)$. The precise value of τ_l depends on the interaction time θ and on the minimum under consideration, but in our dimensionless units $\tau_l\simeq 1$. Converting back to dimensional units, we find that the time it takes to reach an equilibrium photon statistics around a given minimum is of the order of $t_l\simeq\gamma^{-1}$, the damping time of the field in the cavity.

B. Global equilibrium

The local minima of $V(\nu)$ are only metastable. For long enough times, $p(\nu,t)$ will leak away from the neighborhood of any ν_m, which is not the global minimum. We estimate the time scale of this tunneling process by applying the familiar Kramers analysis.[25]

To this end we first introduce a new photon number variable $y=y(\nu)$ through the equation

$$\frac{dy}{d\nu}=\frac{1}{\sqrt{g(\nu)}} . \tag{4.7}$$

It follows easily from (3.15) that in terms of the variables y, τ, and for the new distribution function $p=\sqrt{g}p$, the Fokker-Planck equation becomes

$$\frac{\partial}{\partial\tau}\rho(y,\tau)=-\frac{\partial}{\partial y}\left[\left[\frac{q(y)}{\sqrt{g(y)}}-\frac{1}{4N_{\rm ex}}\frac{g'(y)}{g(y)}\right]\rho(y,\tau)\right] + \frac{1}{2N_{\rm ex}}\frac{\partial^2}{\partial y^2}\rho(y,\tau) . \tag{4.8}$$

As compared with (3.15), this new form of the Fokker-Planck equation presents the distinct advantage of having a constant diffusion coefficient. The new effective potential becomes

$$v(y)=-\int dy\left[\frac{q(y)}{\sqrt{g(y)}}-\frac{1}{4N_{\rm ex}}\frac{g'(y)}{g(y)}\right] =V(\nu)-\frac{1}{4N_{\rm ex}}\ln g(\nu) , \tag{4.9}$$

and the tunneling rate from the minimum $v(y_m)$ of this potential over a subsequent maximum $v(y_M)$ is

$$W=\frac{1}{2\pi}[\,|v''(y_m)v''(y_M)|\,]^{1/2} \times\exp\{-2N_{\rm ex}[v(y_M)-v(y_m)]\} . \tag{4.10}$$

To zeroth order in $N_{\rm ex}$, the extrema of the potential $v(y)$ coincide with the extrema of $V(\nu)$, and at the extrema

$$v''(y)=-q'(\nu) . \tag{4.11}$$

Consequently, the tunneling rate (4.10) is approximately given by

$$W=\frac{1}{2\pi}\left[|q'(\nu_m)|\,|q'(\nu_M)\frac{g(\nu_M)}{g(\nu_m)}\right]^{1/2}$$
$$\times\exp\{-2N_{\rm ex}[V(\nu_M)-V(\nu_m)]\}\ . \tag{4.12}$$

Both the prefactor and the potential difference inside the exponential depend on the interaction time, the minimum ν_m under consideration and the maximum next to ν_m which happens to give the smallest potential difference $V(\nu_M)-V(\nu_m)$. These interrelations could easily be analyzed numerically, but the message of Eq. (4.12) is obvious by inspection: both the potential difference and the prefactor are of order unity in our dimensionless units, thus in the dimensional units the tunneling time behaves qualitatively like

$$t_g\simeq\gamma^{-1}\exp(\alpha N_{\rm ex})\ , \tag{4.13}$$

with α being of order unity. For large atomic fluxes, $N_{\rm ex}\gg 1$, the tunneling time may be extremely long, in which case the metastable states of the microscopic maser are very long lived. But for small $N_{\rm ex}$, it becomes comparable to the intrawell redistribution time t_l.

C. Hysteretic behavior

If in an experiment the pump parameter θ is scanned slowly, e.g., by slowly varying the interaction time $t_{\rm int}$ such that

$$\frac{d\theta}{dt}\ll\gamma\ , \tag{4.14}$$

the photon number distribution will remain in adiabatic equilibrium at the potential minimum where it happens to reside. The values of θ at which the first-order transition in the state of the field take place may then differ significantly from those predicted by the steady-state theory. Moreover, if θ is scanned back and forth, the state of the field can exhibit hysteresis (bistability). An example is provided in Fig. 9, which shows the average photon number in the cavity as obtained from the numerical solution of the Fokker-Planck equation (3.15) when the pump parameter is cycled linearly between two values $\theta=\pi$ and $\theta=4.4\pi$ in a dimensionless time 80γ, for $N_{\rm ex}=100$ and $n_b=0.1$.

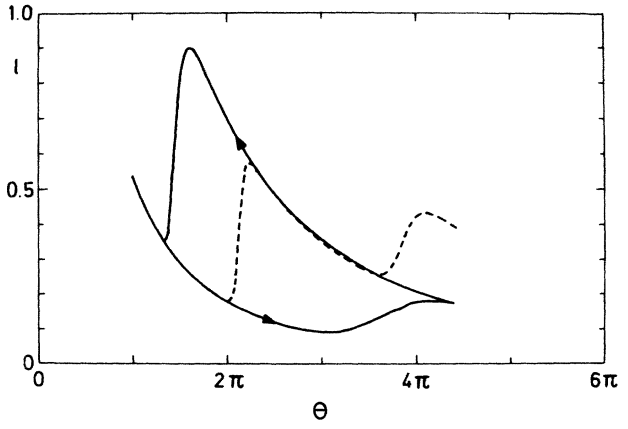

FIG. 9. Hysteresis in the normalized photon number l when scanning the pump parameter θ linearly between the values π and 4.4π in a time of 80γ and back.

V. DISCUSSION

In this paper, we have presented a detailed theory of a truly microscopic maser, and shown that its operation typically differs greatly from that of conventional lasers. In particular, the micromaser is characterized by the appearance of a series of first-order phase transitions following the usual maser threshold, rather than by conventional saturation. It usually emits nonclassical radiation, and above threshold its radiation is not coherent in general. We demonstrated in Sec. II that this fundamental difference between the micromaser and conventional lasers and masers can be traced back to the fact that they do not experience enough stochasticity to erase the quantum-mechanical phases characteristic of coherent, quantum-mechanical light-matter interaction. We showed that if a sufficient amount of noise is added to the system, e.g., in the form of an atomic velocity distribution of of inhomogeneous broadening, then a behavior of the conventional type is recovered. In normal lasers, irreversible spontaneous emission into the continuum of modes of the electromagnetic field always guarantees a smoothing of the quantum-mechanical phases, even in the absence of other sources of noise. In contrast, micromasers are truly single-mode systems, with no irreversible spontaneous emission. The absence of conventional saturation, which is at the origin of the Poissonian photon statistics in normal lasers far above threshold, as well as the sequence of first-order phase transitions already mentioned, are a direct consequence of this fact. In this, the output characteristics of the micromaser can be seen as a signature of inhibited spontaneous emission.

The Fokker-Planck approach of Secs. III and IV provides an alternate, intuitively clear picture of the physics of the micromaser. It indicates that the photon number of the cavity mode evolves to a good approximation according to the equation

$$\dot{n}=R\sin^2(\sqrt{n}\,\kappa t_{\rm int}/2)-\gamma n\ , \tag{5.1}$$

reflecting the competition of pumping and field damping. This equation may have several stable solutions, i.e., several possible metastable states of the micromaser. Again, this is due to the truly coherent nature of atom-single-field mode interaction, which is usually masked when irreversible spontaneous emission and/or other sources of stochasticity are introduced into the system.

Random fluctuations of the photon number due to the quantum discreteness ("granularity")[10] of the atom-field interaction (and the Poissonian arrivals of the atoms, as well as possible velocity distribution of the atoms) prevent the system from converging exactly to the stable stationary solutions of (4.1). Instead, a stochastic photon number distribution around these points is established in a time on the order of the cavity damping time γ^{-1}. The

fluctuations also throw the micromaser between the basins of attraction of the fixed points of (4.1), and these tunneling transitions conspire in such a way that after a long time the maser most likely operates in the particular stationary state that corresponds to the global minimum of the potential $V(v)$.

The microscopic maser is a nontrivial system where the microscopic mechanism of both continuous and first-order phase transitions are effective. Furthermore, by varying the flux of the atoms, a transition from a few-particle system ($N_{ex} \sim 1$) to the thermodynamic limit ($N_{ex} \to \infty$) can in principle be followed experimentally. The micromaser no doubt exhibits some quite interesting statistical mechanics, which remains to be studied. Further, it opens the way to a number of extensions, including the possibility of generating squeezed states of the electromagnetic field if a well defined phase can be imposed on the system, e.g., by injecting atoms in a coherent superposition of upper and lower states.[26]

APPENDIX: STOCHASTIC AVERAGES

In the microscopic theory of Sec. II, the field density matrix of the micromaser is governed by an equation of the type

$$x_{n+1} = L(\xi_n) x_n \ , \tag{A1}$$

where L is a linear operator depending on the random variable ξ_n (either the interval between successive atoms or the interaction time, or both). Our aim is to calculate the average of $x_n(\xi_1, \ldots, \xi_{n-1})$, assuming that the ξ_i are statistically independent.

Since x_n, which now also is a random variable, only depends on $\xi_1, \ldots, \xi_{n-1}$, it is statistically independent of $L(\xi_n)$, and the average of (A1) can be taken simply by factorizing the rhs:

$$\langle x_{n+1}(\xi_1, \ldots, \xi_n) \rangle = \langle L(\xi_n) \rangle \langle x_n(\xi_1, \ldots, \xi_{n-1}) \rangle \ . \tag{A2}$$

This prescription immediately leads to Eqs. (2.8) and (2.19) of the main text.

ACKNOWLEDGMENTS

This work was initiated while all three authors were at the Max-Planck Institute for Quantum Optics in Garching. The part of this project done at the University of Rochester is supported by the U.S. Office of Naval Research and that done at the University of Arizona by the Joint Services Optics Program and by National Science Foundation Grant No. PHY-8603368. We are thankful to Professor J. H. Eberly, Professor H. Haken, Professor P. L. Knight, Professor L. Lugiato, Professor M. O. Scully, and Professor H. Walther for useful discussions.

[1] P. Goy, J. D. Raimond, M. Gross, and S. Haroche, Phys. Rev. Lett. **50**, 1903 (1983).
[2] D. Kleppner, Phys. Rev. Lett. **47**, 233 (1981); R. Hulet and D. Kleppner, *ibid.* **55**, 2137 (1985).
[3] G. Gabrielse and H. Demhelt, Phys. Rev. Lett. **55**, 67 (1985).
[4] P. Dobiasch and H. Walther (unpublished).
[5] For a recent review, see P. Filipovicz, P. Meystre, G. Rempe, and H. Walther, Opt. Acta **32**, 1115 (1985).
[6] E. T. Jaynes and F. W. Cummings, Proc. IEEE **51**, 89 (1963).
[7] F. W. Cummings, Phys. Rev. **140**, 1051 (1965).
[8] P. Meystre, E. Geneux, A. Quattropani, and A. Faist, Nuovo Cimento **25**, 521 (1975).
[9] T. von Foerster, J. Phys. A **8**, 95 (1975).
[10] J. H. Eberly, N. B. Narozhny, and J. J. Sanchez-Mondragon, Phys. Rev. Lett. **44**, 1323 (1980).
[11] D. Meschede, H. Walther, and G. Mueller, Phys. Rev. Lett. **54**, 551 (1985).
[12] G. Rempe and H. Walther (private communication).
[13] In this context, it is useful to remember that the simplest form of the Jaynes-Cummings model does produce squeezed states of the radiation field; see P. Meystre and M. S. Zubairy, Phys. Lett. **89A**, 390 (1982).
[14] For a discussion of squeezed states and their applications, see, e.g., *Quantum Optics, Experimental Gravitation, and Measurement Theory*, edited by P. Meystre and M. O. Scully (Plenum, New York, 1983).
[15] P. Filipowicz, J. Javanainen, and P. Meystre, J. Opt. Soc. Am. B **3**, 906 (1986).
[16] P. Filipowicz, J. Javanainen, and P. Meystre, Opt. Commun. **58**, 327 (1986).
[17] See, e.g., M. Sargent III, M. O. Scully, and W. L. Lamb, Jr., *Laser Physics* (Addison-Wesley, Reading, Mass., 1974).
[18] See, S. M. Barnett and P. L. Knight, Phys. Rev. A **33**, 2444 (1986) for a discussion of this point.
[19] See, e.g., W. H. Louisell, *Quantum Statistical Properties of Radiation* (Wiley, New York, 1973).
[20] The semiclassical counterpart of this result was first obtained by W. E. Lamb, Jr., *Quantum Mechanical Amplifiers*, Vol. 2 of *Lectures in Theoretical Physics*, edited by W. Brittin and D. W. Downs (Interscience, New York, 1960).
[21] P. Meystre, Ph.D. thesis, Swiss Federal Institute of Technology, Lausanne, 1974.
[22] R. J. Glauber, Phys. Rev. **131**, 109 (1963); R. J. Glauber, in *Quantum Optics and Electronics*, edited by C. DeWitt, A. Blandin, and C. Cohen-Tannoudji (Gordon and Breach, New York, 1965).
[23] V. De Giorgio and M. O. Scully, Phys. Rev. A **2**, 1170 (1970); R. Graham and H. Haken, Z. Phys. **237**, 31 (1970).
[24] H. Risken, *The Fokker-Planck Equation, Methods of Solution and Applications*, Vol. 18 of *Springer Series in Synergetics* (Springer-Verlag, Berlin, 1984).
[25] H. A. Kramers, Physica (Utrecht) **7**, 284 (1940).
[26] J. Krause, M. O. Scully, and H. Walther (unpublished).